



HAL
open science

Characterization and optimization of the photoneutron flux emitted by a 6 or 9 MeV electron accelerator for neutron interrogation measurements

Adrien Sari, Frédérick Carrel, Frédéric Lainé

► To cite this version:

Adrien Sari, Frédérick Carrel, Frédéric Lainé. Characterization and optimization of the photoneutron flux emitted by a 6 or 9 MeV electron accelerator for neutron interrogation measurements. *IEEE Transactions on Nuclear Science*, 2018, 65 (9), pp.2539 - 2546. 10.1109/TNS.2018.2857919 . cea-01917842

HAL Id: cea-01917842

<https://cea.hal.science/cea-01917842>

Submitted on 25 Jul 2023

HAL is a multi-disciplinary open access archive for the deposit and dissemination of scientific research documents, whether they are published or not. The documents may come from teaching and research institutions in France or abroad, or from public or private research centers.

L'archive ouverte pluridisciplinaire **HAL**, est destinée au dépôt et à la diffusion de documents scientifiques de niveau recherche, publiés ou non, émanant des établissements d'enseignement et de recherche français ou étrangers, des laboratoires publics ou privés.

Characterization and Optimization of the Photoneutron Flux emitted by a 6 or 9 MeV Electron Accelerator for Neutron Interrogation Measurements

Adrien Sari, Frédéric Carrel, Frédéric Lainé

Abstract—Active neutron interrogation is a non-destructive active method which consists in inducing fission reactions on actinides (^{235}U and ^{239}Pu for instance) and then in detecting prompt and delayed particles emitted further to these reactions. This method is required in various application fields such as radiological characterization of nuclear waste packages and Homeland Security. Neutron sources traditionally used in neutron interrogation facilities are deuterium-tritium neutron generators. However, a linear electron accelerator (LINAC) can also be used as a photoneutron generator. When accelerating electrons with an energy lower than 10 MeV, the use of a secondary target such as heavy water is of interest to convert Bremsstrahlung photons to neutrons and to improve neutron production.

In this paper, we characterize the photoneutron flux emitted by a Linatron-M9 VARIAN LINAC and the photoneutron flux emitted by a secondary target made of heavy water. We show that, operating the LINAC at 9 MeV, the average emission intensity reaches 1.08×10^{10} neutrons per second, which is on the order of ten times higher than the maximum average emission intensity delivered by a traditional deuterium-tritium neutron generator. Then, we carry out neutron interrogation measurements on uranium samples using the Linatron-M9 LINAC and a secondary target made of different volumes of heavy water. We show that prompt neutron signals were enhanced when using 16 kg of heavy water and operating the LINAC at 9 MeV. Performances of the setup were then assessed by carrying out measurements on a mock-up of nuclear waste drum containing different types of matrices. Considering a 0.22 g/cm^3 iron matrix and a uranium sample at the center of the drum, 44 mg of ^{235}U can be detected in five minutes of irradiation time using a single detection block housing five 150NH100 ^3He detectors.

Index Terms—Photoneutron, active neutron interrogation, electron accelerator, LINAC, uranium, nuclear waste packages

I. INTRODUCTION

ACTIVE neutron interrogation is a non-destructive active method which consists in inducing fission reactions on actinides (^{235}U and ^{239}Pu for instance) and then in detecting prompt and delayed particles emitted further to these reactions [1]-[4]. This method is required in various application fields such as radiological characterization of nuclear waste packages and Homeland Security. Indeed, Special Nuclear Material (SNM) such as ^{235}U and ^{239}Pu could potentially be used to make

a nuclear bomb which could be involved in a terrorist attack. Detection of SNM in cargo containers could then be carried out by neutron interrogation. Moreover, many nuclear waste packages can be characterized using neutron interrogation when passive techniques reach their limitations.

Neutron sources traditionally used in neutron interrogation facilities are deuterium-tritium neutron generators [5]. However, a linear electron accelerator (LINAC) can also be used as a neutron generator [6]-[10]. First, electrons are converted into high-energy photons by *Bremsstrahlung* using a conversion target (primary target) made of heavy nuclei material (such as tungsten or tantalum). Secondly, high-energy photons can interact by photonuclear reactions with heavy nuclei and generate neutrons commonly referred to as “photoneutrons”. Photonuclear reaction thresholds are roughly around 7 MeV for tungsten and tantalum isotopes. Considering a LINAC accelerating electrons with an energy lower than 10 MeV, a secondary target would be of interest to convert Bremsstrahlung photons to photoneutrons in order to optimize neutron production and operate the LINAC as neutron source. The two best candidates to be considered as secondary targets are beryllium (^9Be) and heavy water (deuterium oxide, D_2O). Indeed, (γ, n) photonuclear reaction energy thresholds are 1.67 MeV for ^9Be and 2.2 MeV for deuterium.

Thus, an electron accelerator could enable to perform not only photon interrogation and high-energy imaging but also neutron interrogation. With a view to characterizing nuclear waste packages, neutron interrogation could be focused on the detection of fissile actinides whereas photon interrogation could be focused on the detection of both fissile and fertile actinides. High-energy imaging would provide information on the matrix and help to interpret results of neutron and photon interrogation measurements.

However, the use of photoneutrons as interrogative particles to perform neutron interrogation measurements requires first an accurate knowledge of photoneutron flux characteristics [11], and optimization of the photoneutron flux in a second step [12]. In this paper, we characterize the photoneutron flux emitted by a 6 or 9 MeV LINAC. Then, we characterize the photoneutron flux emitted by a secondary target made of heavy water. Subsequently, we optimize the photoneutron flux based on neutron interrogation measurements carried out on uranium

samples with a 6 or 9 MeV LINAC and a secondary target made of heavy water according to two main parameters: electron energy and heavy water volume. Finally, we assess performances of neutron interrogation on a mock-up of nuclear waste package. Different types of fittings (or matrices) have been tested.

In the following of this paper, error bars are shown on experimental results when larger than symbols and MCNP6 simulation results are always under 5% of statistical error. Moreover, concerning experimental data, we conducted each measurement at least three times showing a satisfactory reproducibility.

II. CHARACTERIZATION OF THE PHOTONEUTRON FLUX EMITTED BY A LINATRON-M9 VARIAN LINAC

We characterized the photoneutron flux emitted by a Linatron-M9 VARIAN LINAC housed at the SAPHIR facility [13]-[15] which is located at CEA Saclay (France). Fig. 1 shows the LINAC.

A. Characterization method

The method used in the frame of this photoneutron characterization study has been used in a previous work [11] and is based on three steps. The first step consists in carrying out neutron activation measurements. The neutron activation detector designed in this prior work has been used to measure photoneutrons emitted by the Linatron-M9 LINAC. Fig. 2 shows the photoneutron activation detector, which is composed of a foil of vanadium or aluminum, and polyethylene surrounded by cadmium. Dimensions of the foil are the following: $10.0 \times 10.0 \times 0.1 \text{ cm}^3$. The nuclear reactions of interest are $^{51}\text{V}(n, \gamma)^{52}\text{V}$ and $^{27}\text{Al}(n, \gamma)^{28}\text{Al}$. The second step consists in designing a simulation model of the LINAC using the MCNP6 Monte-Carlo code [16] and taking into account the photonuclear reaction cross-sections from the ENDF/B-VII.1 database [17]. The last step consists in comparing experimental and simulation results regarding the gamma net peak area which signs decay of the ^{52}V or ^{28}Al radioactive nuclei [11].



Fig. 1. Linatron-M9 VARIAN LINAC at the SAPHIR facility (CEA Saclay, France).



Fig. 2. Neutron activation detector [11] in open position.

B. Measurement methodology

The measurement methodology is based on two steps. The first step consists in irradiating the activation detector. These irradiations were carried out operating the LINAC at 9 MeV and 100 Hz during 10 minutes. Two positions of irradiation have been tested, inside and outside the photon field. Fig. 3 shows a scheme of the irradiation setup. Half-lives of ^{52}V and ^{28}Al are respectively 3.74 minutes and 2.24 minutes [11]. As ^{52}V decays emitting a gamma ray at 1474 keV and ^{28}Al decays emitting a gamma ray at 1778 keV, the second step consists in acquiring decay gamma spectra, after 3 minutes of cooling time, using a high purity germanium detector (HPGe) during 10 minutes. An ORTEC GMX35P4-70-PLUS HPGe detector was used (n-type, relative efficiency of 35%). Fig. 4 illustrates acquisition of a decay gamma spectrum.

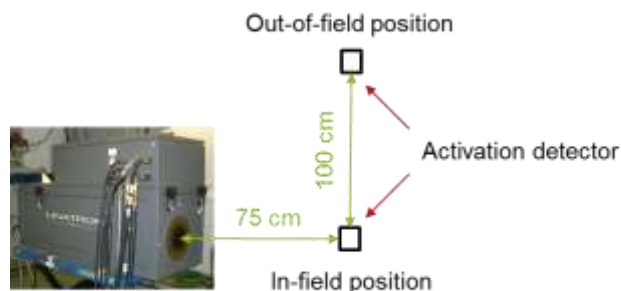


Fig. 3. Scheme of the irradiation setup (not to scale).



Fig. 4. Decay gamma spectrum acquisition step.

C. Results and discussion

Table I shows results obtained. When the activation detector is irradiated in the photon field position, spurious photoneutrons are produced by photonuclear reactions in the cadmium envelope surrounding the activation detector. MCNP6 simulations carried out with and without photonuclear reactions in the cadmium envelope showed that these spurious photoneutrons account for 26% of the signal. Considering the out-of-field position, simulation underestimates experiment by a factor on the order of ten. Moreover, MCNP6 simulations enabled to show that photoneutrons are produced in both the collimator and the conversion target of the LINAC, which are both made of tungsten. The gap between simulation and experimental results is likely to be due to undervaluation of tungsten photonuclear reaction cross-sections in the energy range of interest.

TABLE I

RATIO BETWEEN SIMULATION AND EXPERIMENTAL RESULTS OBTAINED WITH THE ACTIVATION DETECTOR POSITIONED IN OR OUT OF THE PHOTON FIELD

	In-field position	Out-of-field position
V	0.20	0.13
Al	0.13	0.04
Mean value	0.16	0.09

In 2011, K. Kosako *et al.* concluded that, in the energy range from 18 to 38 MeV, tungsten photonuclear reaction cross-sections are undervalued [18]. In 2013, we lead to the same conclusion working in the energy range from 14 to 17 MeV [11]. This new study enables to evaluate how strong is the impact of poor knowledge of tungsten photonuclear reaction cross-sections at 9 MeV near the threshold (roughly around 7 MeV). Reevaluation of tungsten photonuclear reaction cross-sections is required. In the meantime, production of photoneutrons using a secondary target is a possible alternative to avoid the simulation problems encountered with tungsten at 9 MeV.

III. CHARACTERIZATION OF THE PHOTONEUTRON FLUX EMITTED BY A SECONDARY TARGET MADE OF HEAVY WATER

Two types of secondary targets, beryllium and heavy water (deuterium oxide), could be used to produce photoneutrons. ^9Be has a (γ, n) photonuclear reaction energy threshold at 1.67 MeV whereas deuterium has an energy threshold at 2.2 MeV. However, as beryllium is strongly toxic, heavy water has been chosen as secondary target to carry out experiments at the SAPHIR facility. Two different setups have been tested.

A. Setup No. 1

We characterized the photoneutron flux emitted by a secondary target made of heavy water (deuterium oxide, 99.9% purity) positioned in the photon field. This secondary target has a mass of 4 kg, a density of 1.107 g/cm^3 , and the following dimensions: $13.6 \times 13.6 \times 19.6 \text{ cm}^3$. The activation detector

was set in an out-of-field position with either a vanadium or an aluminum foil. Fig. 5 shows a scheme of the irradiation setup. Measurements were carried out for two electron energies: 6 MeV and 9 MeV. Other parameters of the measurement protocol are similar to the ones used previously in this study.

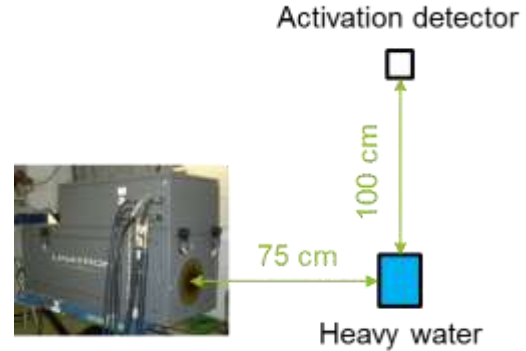


Fig. 5. Scheme of the irradiation setup No. 1 (scheme not to scale).

Average photoneutron emission intensities and energy spectra have been calculated based on MCNP6 simulations for the two electron energies. Average emission intensities were obtained by multiplying the neutron currents integrated on the six surfaces of the secondary target (number of neutrons produced per electron, MCNP6 statistical uncertainties lower than 0.01%) by the number of electrons delivered by the accelerator per second (electron peak current of 100 mA equivalent to 6.25×10^{17} electrons per second), by the pulse duration (2.5 μs), and by the frequency (100 Hz). The average emission intensities reach 3.39×10^8 neutrons per second at 6 MeV and 1.36×10^9 neutrons per second at 9 MeV. Neutron currents were also calculated with MCNP6 on the six surfaces of the secondary target using 1 keV energy bins to determine the neutron energy spectra. Results obtained are shown in Fig. 6. The mean neutron energy is 0.5 MeV for 6 MeV electrons and 0.8 MeV for 9 MeV electrons.

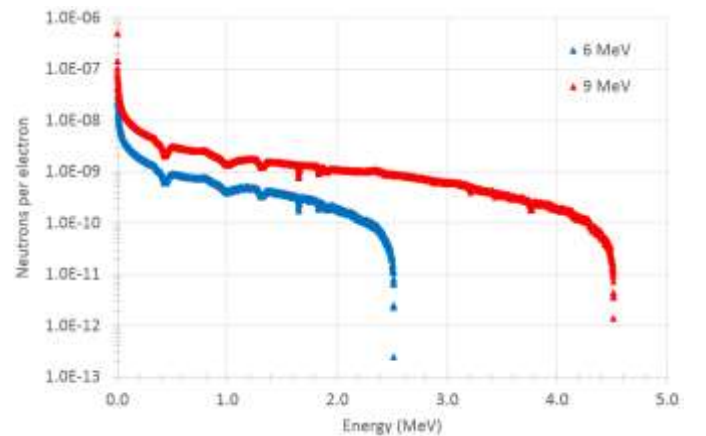


Fig. 6. Energy spectra of neutrons emitted by the 4 kg heavy water secondary target calculated with MCNP6 for two electron energies.

Table II gathers results obtained with the first setup. Simulation still underestimates experiment, which could be explained by the fact that facility environment has not been simulated due to complex geometry and calculation time limits.

A second setup has then been tested in order to further reduce the gap between simulation and experimental results.

TABLE II

RATIO BETWEEN SIMULATION AND EXPERIMENTAL RESULTS OBTAINED WITH SETUP NO. 1

	6 MeV	9 MeV
V	0.36	0.51
Al	0.14	0.16
<i>Mean value</i>	<i>0.25</i>	<i>0.34</i>

B. Setup No. 2

The aim of the second setup, shown in Fig. 7, was to avoid impact of backscattered neutrons in the facility environment using a neutron interrogation cell designed in a previous study [19] and shown in Fig. 8. The cell is made of 0.95 g/cm³ polyethylene, walls are 5 cm thick and internal dimensions are 70 × 90 × 92 cm³. Using the same activation measurement protocol as the one used with the first setup, we characterized the photoneutron flux emitted by a secondary target made of heavy water. In this setup, the secondary target has a mass of 16 kg, a density of 1.107 g/cm³ and the following dimensions: 54.4 × 13.6 × 19.6 cm³. Vanadium or aluminum foils were not positioned in the neutron activation detector but placed directly in the neutron interrogation cell (outside the photon field) as shown in Fig. 8.

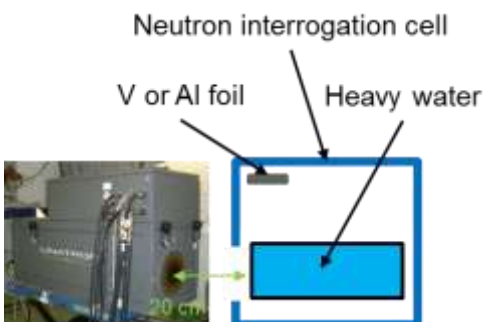


Fig. 7. Scheme of the irradiation setup No. 2 (scheme not to scale).

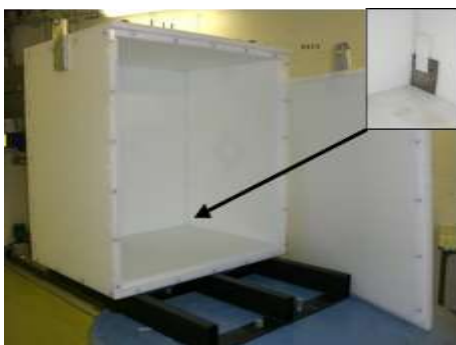


Fig. 8. Neutron interrogation cell (in open position) and foil position in irradiation setup No. 2.

Using the same calculation methodology as the one described previously, average photoneutron emission intensities and

energy spectra have been calculated for the two electron energies and the LINAC operated at 100 Hz. Average emission intensities reach 2.03×10^9 neutrons per second at 6 MeV and 7.99×10^9 neutrons per second at 9 MeV. Neutron energy spectra are shown in Fig. 9. The mean neutron energy is 0.4 MeV for 6 MeV electrons and 0.7 MeV for 9 MeV electrons.

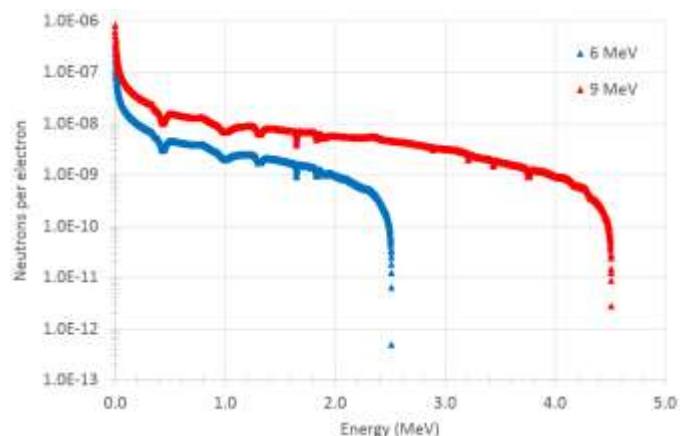


Fig. 9. Energy spectra of neutrons emitted by the 16 kg heavy water secondary target calculated with MCNP6 for two electron energies.

Table III gathers results obtained with the second setup, which enabled to reduce the gap between simulation and experimental results compared to the first setup. Simulation underestimates experiment by a factor of two at 6 MeV and by 26% at 9 MeV. The residual discrepancies between simulation and experimental results could be explained by two possible causes:

- firstly, inaccuracy of (γ, n) photonuclear reaction cross-sections for deuterium;
- secondly, the widths of the 6 MeV and 9 MeV electron energy spectra delivered by the LINAC are not taken into account in the MCNP6 calculations due to lack of information.

With a view to estimating the experimental neutron emission, ratios presented in Table III are used to scale photoneutron emission calculated previously, leading to 4.05×10^9 neutrons per second at 6 MeV and 1.08×10^{10} neutrons per second at 9 MeV (uncertainties around 5%). It is important to emphasize the fact that the values of average emission intensities are comparable to the highest neutron yields delivered by deuterium-tritium generators currently on the market (10^{10} neutrons per second for the GENIE 35 neutron generator designed by EADS Sodern and for the DT110 manufactured by Adelphi technology for instance). Higher average emission intensities would enable to expand detection limits for neutron interrogation measurements.

TABLE III

RATIO BETWEEN SIMULATION AND EXPERIMENTAL RESULTS OBTAINED WITH SETUP NO. 2

	6 MeV	9 MeV
V	0.48	0.73
Al	0.51	0.75
Mean value	0.50	0.74

IV. OPTIMIZATION OF THE PHOTONEUTRON FLUX FOR NEUTRON INTERROGATION MEASUREMENTS

We optimized the photoneutron flux delivered by a secondary target made of heavy water and assessed performances obtained in neutron interrogation measurements using the Linatron-M9 VARIAN LINAC housed at the SAPHIR facility.

A. Experimental setup

Basically, the experimental setup is composed of the Linatron-M9 LINAC, a secondary target of heavy water, the neutron interrogation cell [19], a sample of uranium positioned outside of the photon beam (in order to avoid photofission reactions), and a detection block. This block has the following external dimensions $120 \times 26.5 \times 12.5$ cm³ and is equipped with five 150NH100 ³He detectors (one meter long, one inch in diameter, 4 bars of pressure) embedded in polyethylene and covered by a 1 mm thick cadmium foil. The experimental setup is shown in Fig. 10. Uranium samples used for these experiments have a cylindrical shape, are enriched between 2.8% and 9.6%, and have total masses of a few grams.



Fig. 10. Neutron detection block containing five ³He detectors positioned against the neutron cell.

B. Measurement protocol

Measurements were carried out while operating the LINAC emitting either 6 or 9 MeV electrons at 50 Hz. Different masses of heavy water have been tested: 4 kg and 16 kg. Measurements have also been conducted without heavy water in order to estimate contribution from photoneutrons emitted by the LINAC on neutron interrogation measurements. Moreover, uranium samples have been interrogated with and without a

1 mm thick cadmium envelope around them in order to estimate relative contributions from thermal and fast fission reactions (thermal neutrons are cut by cadmium).

Total irradiation time was chosen to be 5 minutes. Prompt neutrons were detected between 2 and 8 ms after the electron pulse whereas delayed neutrons were detected between 14 and 20 ms after the pulse. Fig. 11 shows an example of neutron counting time histogram. The signal obtained when the sample is surrounded by cadmium is superimposed with background, showing that interrogation is mainly due to thermalized photoneutrons.

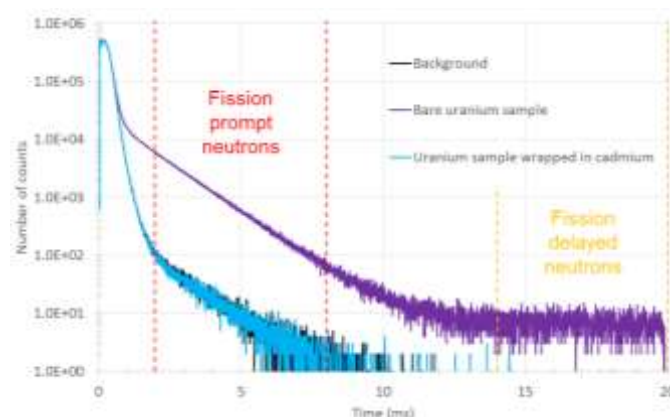


Fig. 11. Neutron counting time histogram obtained for a 9.6% enriched uranium sample irradiated during 5 minutes with 16 kg of heavy water using the Linatron-M9 operated at 9 MeV and 50 Hz.

C. Prompt neutron signal

Fig. 12 shows prompt neutron signals obtained for different ²³⁵U masses using either secondary targets of 4 kg or 16 kg of heavy water, and also without secondary target. For these measurements, the LINAC was set at 9 MeV. Contribution from photoneutrons emitted by the LINAC can be neglected. Signals measured are more than twice higher when using a heavy water secondary target of 16 kg in comparison with the 4 kg target. This tendency is in agreement with additional MCNP6 simulation results, which showed that half of the photoneutron flux from the 16 kg heavy water secondary target is emitted by the first quarter facing the LINAC. Consistently, experiments show that the photoneutron flux emitted by the 16 kg heavy water secondary target is twice higher in comparison with the photoneutron flux emitted by the 4 kg heavy water secondary target.

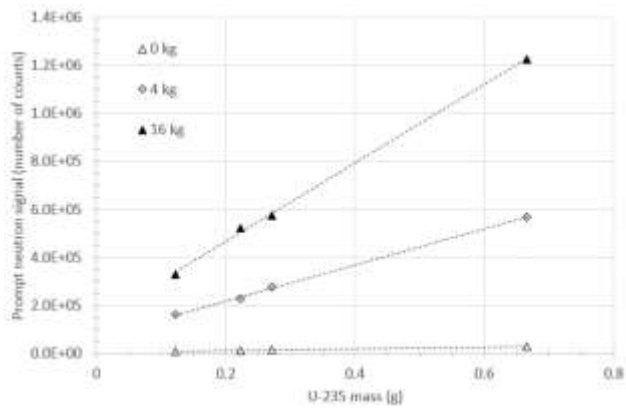


Fig. 12. Prompt neutron signals as a function of ^{235}U mass obtained with different heavy water volumes at 9 MeV.

Fig. 13 shows prompt neutron signals obtained for different ^{235}U masses using either the LINAC at 6 or 9 MeV. These measurements were conducted using a secondary target of 16 kg of heavy water. Sensitivity is more than twice higher when setting the LINAC at 9 MeV rather than 6 MeV.

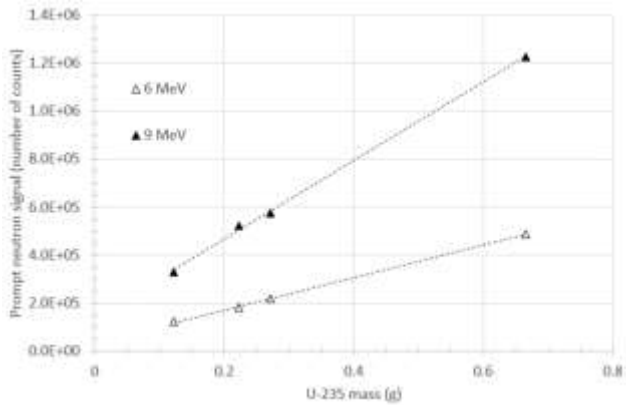


Fig. 13. Prompt neutron signals as a function of ^{235}U mass obtained for two electron energies with the 16 kg heavy water target.

V. PERFORMANCES FOR NUCLEAR WASTE PACKAGES

We assessed performances of the neutron interrogation measurement setup at the SAPHIR facility using 220 liter nuclear waste mock-up drums with 82 cm of height, 60 cm of diameter, and a steel wall thickness of 1 mm.

A. Experimental setup

The setup, shown in Fig. 14, is similar to the one described previously. Measurements were carried out with the optimized photoneutron flux, that is to say setting electron energy at 9 MeV and using a 16 kg heavy water secondary target. A mock-up drum was positioned in the cell and outside the photon beam in order to avoid photofission reactions. The uranium samples were positioned at the center of mock-up drums containing different fittings: empty drum; vinyl matrix of 0.02 g/cm^3 average density; iron matrix of 0.22 g/cm^3 average density. The vinyl and iron matrices are shown in Fig. 15.



Fig. 14. Experimental setup (back of the neutron cell in open position).



Fig. 15. Mock-up drums with central pipe allowing insertion of uranium samples. On the left: vinyl matrix of 0.02 g/cm^3 average density. On the right: iron matrix of 0.22 g/cm^3 average density.

B. Experimental results

Impact of matrices on prompt neutron signals has been studied. Fig. 16 shows prompt neutron signals obtained as a function of ^{235}U mass for the three different measurement configurations. The lowest sensitivity is obtained with the 0.22 g/cm^3 iron matrix, which can be explained by the fact that the vinyl matrix has a very low density of 0.02 g/cm^3 . Mass detection limits were calculated from the prompt neutron signals [13] for an irradiation time of five minutes:

- empty drum: 17 mg of ^{235}U ;
- drum with 0.02 g/cm^3 vinyl matrix: 27 mg of ^{235}U ;
- drum with 0.22 g/cm^3 iron matrix: 44 mg of ^{235}U .

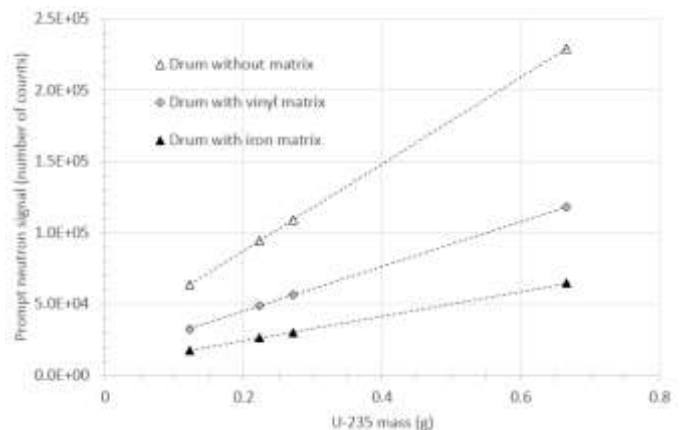


Fig. 16. Prompt neutron signals as a function of ^{235}U mass obtained for the three measurement configurations.

Impact of matrices on delayed neutron signals has also been studied. Fig. 17 shows delayed neutron signals obtained as a function of ^{235}U mass for the three different measurement configurations. We can notice that sensitivities obtained with the 0.22 g/cm^3 iron matrix and the 0.02 g/cm^3 vinyl matrix are almost identical for delayed neutrons whereas they are significantly different for fast neutrons. Sensitivity is proportional to the product between the fission rate in the uranium sample and the prompt or delayed neutron detection efficiency. For either the vinyl or iron matrix, the difference between sensitivities for prompt and delayed neutrons is only due to neutron detection efficiency. Mean energies of prompt and delayed neutrons are respectively around 2 MeV and 0.5 MeV. The detection efficiency for delayed neutrons emitted by the uranium sample placed at the center of the drum is more impacted in the case of the vinyl matrix which contains hydrogenous material than in the case of the iron matrix.

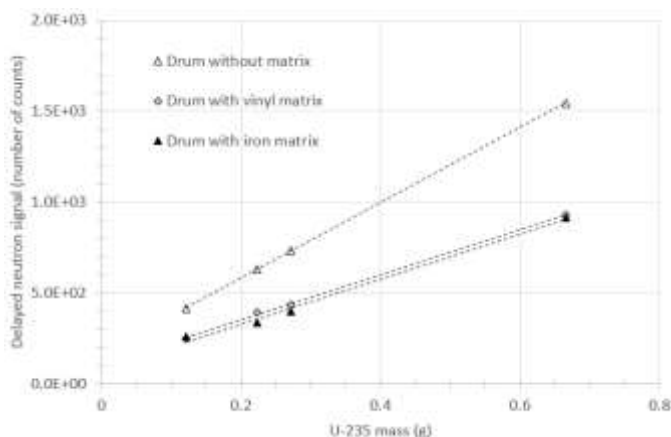


Fig. 17. Delayed neutron signals as a function of ^{235}U mass obtained for the three measurement configurations.

With the aim of improving characterization of fissile material and distinguishing uranium from plutonium contributions, it is expected that ratios between prompt and delayed neutron signals might enable to differentiate ^{235}U from $^{239+241}\text{Pu}$ [1]. Therefore, the impact of the three matrices on this ratio has been investigated. Fig. 18 presents ratios between prompt and delayed neutron signals obtained as a function of ^{235}U mass, and shows that matrix impact is significant. The value of the ratio depends on the matrix because of differences between prompt and delayed neutron mean energies and consequently prompt and delayed neutron detection efficiencies. Fig. 18 illustrates how important is knowledge of the matrix contained in a nuclear waste package, thereby proving the need for high-energy imaging which can be performed with the photon beam produced by a LINAC.

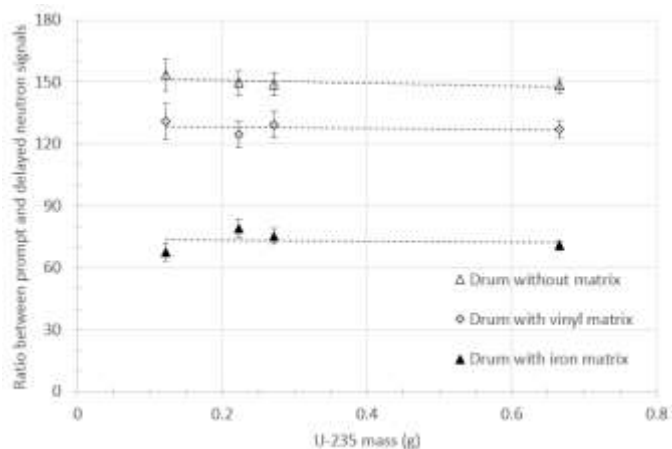


Fig. 18. Ratio between prompt and delayed neutron signals as a function of ^{235}U mass obtained for the three measurement configurations.

VI. SUMMARY AND PROSPECTS

This study is part of a long-term roadmap aiming at designing a new platform dedicated to nuclear waste packages characterization based on a LINAC which would enable to perform complementary characterization techniques such as photon interrogation, neutron interrogation, and high-energy imaging. MCNP6 simulation underestimates photoneutron production due to poor knowledge of tungsten photonuclear reaction cross-sections near the energy threshold, which is around 7 MeV. The gap between simulation and measurement reached approximately one decade. Reevaluation of tungsten photonuclear reaction cross-sections is then required. A secondary target made of heavy water has been chosen as photoneutron source as the deuterium photonuclear reaction cross-section is better known, with an energy threshold of 2.2 MeV. As a result, underestimation of photoneutron production by simulation decreased to a factor of two at 6 MeV and 26% at 9 MeV.

Average emission intensities with 16 kg of heavy water and an electron pulse frequency of 100 Hz have been estimated to 4.05×10^9 neutrons per second at 6 MeV and 1.08×10^{10} neutrons per second at 9 MeV (uncertainty around 5%). Higher average emission intensities can be reached by increasing the pulse frequency of the LINAC. However, a trade-off must be found between frequency and interpulse period in order to enable detection of prompt and delayed neutrons between pulses.

Neutron interrogation measurements on uranium samples have then been performed with a LINAC emitting 9 MeV electrons and a secondary target made of 16 kg of heavy water. Performances were assessed by carrying out measurements on a mock-up of 220 liter nuclear waste drum containing different matrices. Considering a 0.22 g/cm^3 iron matrix and the sample at the center of the drum, the prompt neutron detection limit is 44 mg of ^{235}U in five minutes of irradiation time using a single detection block housing only five $150\text{NH}100\text{ }^3\text{He}$ detectors.

Further, new measurements could be carried out in order to test other types of matrices and evaluate performances obtained when placing samples at different positions in the mock-up drum. With a view to improving nuclear waste packages characterization, combination of the three measurement techniques that can be implemented sequentially with a same

LINAC, namely high-energy imaging, photon interrogation and neutron interrogation, should be further investigated.

REFERENCES

- [1] A.-C. Raoux *et al.*, "Transuranic waste assay by neutron interrogation and online prompt and delayed neutron measurement," *Nucl. Instrum. Methods Phys. Res. B*, vol. 207, pp. 186-194, 2003.
- [2] L. Lakosi, C. Tam Nguyen, J. Bagi, "Photoneutron interrogation of low-enriched uranium induced by Bremsstrahlung from a 4 MeV linac," *Nucl. Instrum. Methods Phys. Res. B*, vol. 266, pp. 295-300, 2008.
- [3] L. Lakosi, C. Tam Nguyen, E. Serf, "Neutron interrogation of shielded/unshielded uranium by a 4 MeV linac," *Appl. Radiat. Isot.*, vol. 69, pp. 1251-1254, 2011.
- [4] F. Jallu, C. Passard, E. Brackx, "Application of active and passive neutron non destructive assay methods to concrete radioactive waste drums," *Nucl. Instrum. Methods Phys. Res. B*, vol. 269, pp. 1956-1962, 2011.
- [5] A. Mariani, C. Passard, F. Jallu, and H. Toubon, "The help of simulation codes in designing waste assay systems using neutron measurements methods; Applications to the alpha low level waste assay system PROMETHEE 6," *Nucl. Instrum. Methods Phys. Res. B*, vol. 211, pp. 389-400, 2003.
- [6] L.A. Franks, *et al.*, "High sensitivity transuranic waste assay by simultaneous photon and thermal-neutron interrogation using an electron linear accelerator," *Nucl. Instrum. Methods Phys. Res.*, vol. 193, pp. 571-576, 1982.
- [7] V.L. Chakhlov, Z.W. Bell, V.M. Golovkov, M.M. Shtein, "Photoneutron source based on a compact 10 MeV betatron," *Nucl. Instrum. Methods Phys. Res. A*, vol. 422, pp. 5-9, 1999.
- [8] F. Jallu *et al.*, "The simultaneous neutron and photon interrogation method for fissile and non-fissile element separation in radioactive waste drums," *Nucl. Instrum. Methods Phys. Res. B*, vol. 170, pp. 489-500, 2000.
- [9] L. Lakosi, C. Tam Nguyen, "Neutron interrogation of high-enriched uranium by a 4 MeV linac," *Nucl. Instrum. Methods Phys. Res. B*, vol. 266, pp. 3295-3301, 2008.
- [10] A. Sari *et al.*, "Detection of actinides with an electron accelerator by active photoneutron interrogation measurements," *IEEE Trans. Nucl. Sci.*, vol. 59, no. 3, pp. 605-611, 2012.
- [11] A. Sari *et al.*, "Characterization of the photoneutron flux emitted by an electron accelerator using an activation detector," *IEEE Trans. Nucl. Sci.*, vol. 60, no. 2, pp. 693-700, 2013.
- [12] A. Sari, F. Carrel, C. Jouanne, A. Lyoussi, O. Petit, "Optimization of the photoneutron flux emitted by an electron accelerator for neutron interrogation applications using MCNPX and TRIPOLI-4 Monte Carlo codes," *Proceedings of IPAC2013*, pp. 3630-3632
- [13] M. Gmar *et al.*, "Assessment of actinide mass embedded in large concrete packages by photon interrogation and photofission," *Appl. Radiat. Isot.*, vol. 63, pp. 613-619, 2005.
- [14] F. Carrel *et al.*, "Measurement of plutonium in large concrete radioactive waste packages by photon activation analysis," *IEEE Trans. Nucl. Sci.*, vol. 57, no. 6, pp. 3687-3693, 2010.
- [15] A. Sari *et al.*, "Neutron interrogation of actinides with a 17 MeV electron accelerator and first results from photon and neutron interrogation non-simultaneous measurements combination," *Nucl. Instrum. Methods Phys. Res. B*, vol. 312, pp. 30-35, 2013.
- [16] T. Goorley *et al.*, "Initial MCNP6 release overview," *Nuclear Technology*, vol. 180, no. 3, pp. 298-315, 2012.
- [17] Database ENDF/B-VII.1 [online]. Available: <http://www.nndc.bnl.gov/exfor/endl.htm>
- [18] K. Kosako *et al.*, "Angular distribution of photoneutrons from copper and tungsten targets bombarded by 18, 28, and 38 MeV electrons," *J. Nucl. Sci. Technol.*, vol. 48, pp. 227-236, 2011.
- [19] A. Sari *et al.*, "Design of a neutron interrogation cell based on an electron accelerator and performance assessment on 220 liter nuclear waste mock-up drums," *IEEE Trans. Nucl. Sci.*, vol. 61, no. 4, pp. 2144-2148, 2014.